2023 IEEE Conference on Control Technology and Applications (CCTA)
August 16-18, 2023. Bridgetown, Barbados

Motion Planning of Articulated Vehicles with Active Trailer Steering by Particle Filtering

Hassan Iqbal, Stefano Di Cairano, Karl Berntorp

2023 IEEE Conference on Control Technology and Applications (CCTA) | 979-8-3503-3544-6/23/$31.00 ©2023 IEEE | DOI: 10.1109/CCTA54093.2023.10253020

***Abstract*— This paper proposes a method for motion planning of tractor-trailer combinations having active trailer steering. Autonomous driving (AD) in structured environments involves a set of predefined requirements that the vehicle should satisfy, such as lane following, safety distances to surrounding obstacles, speed preferences, or ride smoothness. We have previously shown that by interpreting the motion-planning problem as a nonlinear, non-Gaussian estimation problem, we can leverage particle filtering to efficiecntly determine suitable vehicle trajectories satisfying such requirements. In this paper, we extend the motion planner to determine safe and drivable trajectories for semi-trailer articulated vehicles in scenarios requiring complex maneuvers. In a closed-loop simulation study, the trajectories are tracked with a few centimeter accuracy, validating dynamic feasibility of the proposed method.**

I. INTRODUCTION

While fully AD-capable vehicles are still mostly at the research and development stage, production vehicles are commonly being equipped with advanced driver-assistance systems (ADAS), such as adaptive cruise control and lane-change assist. Passenger vehicles with autonomous driving (AD) capabilities are increasingly being tested on public roads, even with commercialization plans in the near future, e.g., in the transportation sector. This is driven by both safety and economic aspects, such as the high number of traffic accidents associated with overtaking and lane-change maneuvers, potential fuel savings, and labor shortage [1].

The emergence of articulated vehicles such as (long) tractor-trailer combinations has led to reduced costs for goods transportation and reduced fuel consumption, and thereby decreased environmental footprint. However, tractor-trailer combinations have decreased maneuverability, particularly in urban areas where, e.g., performing 90-deg turns in intersections and maneuvering roundabouts are two common tasks that are made more difficult with an articulated vehicle and related to the *swept path*, which is larger for articulated vehicles [2]. The swept path is defined by the outer path of the tractor front wheel axle and the path of the center of the trailer wheel axle. Also, the kinematics of articulated vehicles are significantly different from non-articulated ones. This creates additional challenges from a control and planning perspective, such as the risk of jackknifing, and how to reverse and navigate narrow streets and turns [3], [4]. One solution to improve maneuverability of articulated vehicles is to have active trailer steering, in addition to the conventional tractor steering. While this idea has been around since the 1930's, recently, several methods for trajectory tracking have been developed, see, e.g., [5].

Mitsubishi Electric Research Laboratories (MERL), 02139 Cambridge, MA, USA, Email: karl.o.berntorp@ieee.org

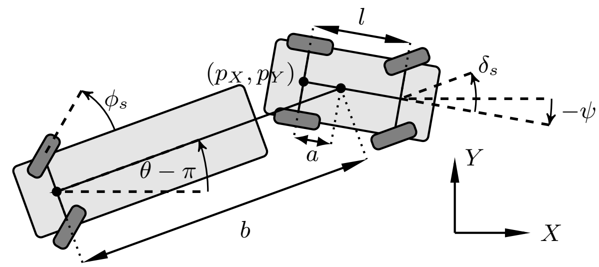

Fig. 1. Schematic of the considered articulated vehicle geometry and related notation.

Here, we extend our previously developed particle filter (PF) based motion-planning approach for automated cars to compute motion plans for articulated vehicles comprising a tractor-trailer setup with active trailer steering. Particle filtering is a sampling-based technique for solving nonlinear estimation problems. PFs numerically approximate the probability density function (PDF) of the variables of interest given the measurement history, by generating random trajectories and assigning a weight to them according to how well they predict the observations. The driving requirements, such as staying on the road, right-hand traffic, and obstacle avoidance, are known ahead of planning, and we formulate the driving requirements as measurements generated by an ideal system. We demonstrate that, with suitable modifications, our planner can produce feasible motion plans also for articulated vehicles with active trailer steering. Our method also reduces the swept path compared to passive trailers, a key consideration for tractor-trailer combinations [2].

Approaches for motion planning of passenger vehicles relying on model predictive control (MPC) have been developed for specialized scenarios [6], [7]. However, a typical limiting factor with these approaches is nonconvexity. This results in achieving only a locally optimal solution, which may be significantly far from the globally optimal one. Motion planning in autonomous vehicle research is often performed using either sampling-based methods such as rapidly-exploring random trees (RRTs) [8], [9], graph-search methods [10], [11] such as A* or D* [12], [13] to get a global solution, possibly using MPC for a local refinement of the motion plan and for tracking [14], [15].

Most motion-planning methods have been developed for passenger cars but there has been some work tailoring motion-planning methods for improved performance and safety. E.g., [16] leverages optimization-based techniques for path planning of articulated vehicles on narrow streets,

[17] considers the motion-planning problem for reversing by adapting the closed-loop RRT, and [18] considers tractor-trailer path planning in semi-structured environments. While our method is sampling based as [17], it is based on estimation theory and as such naturally can include environment and modeling uncertainty. Furthermore, because unlike [18] our method is designed for structured scenarios, it generates control inputs according to predefined stochastic requirements rather than states, and therefore is less susceptible to the dimensionality issues due to the increasingly complex models associated with articulated vehicles.

Notation: Throughout, $\boldsymbol{y}_{m:k} := \{\boldsymbol{y}_m, \dots, \boldsymbol{y}_k\}$, $p(\boldsymbol{x}_{0:k}|\boldsymbol{y}_{0:k})$ denotes the conditional probability density function of the state trajectory $\boldsymbol{x} \subset \mathcal{X} \in \mathbb{R}^{n_x}$ at time $t_k \in \mathbb{R}$ conditioned on the measurement $\boldsymbol{y} \subset \mathcal{Y} \in \mathbb{R}^{n_y}$ from time t_0 to time t_k. Given mean vector $\boldsymbol{\mu}$ and covariance matrix $\boldsymbol{\Sigma}$, $\mathcal{N}(\boldsymbol{\mu}, \boldsymbol{\Sigma})$ and $\mathcal{N}(\boldsymbol{x}|\boldsymbol{\mu}, \boldsymbol{\Sigma})$ stand for the Gaussian distribution and PDF, respectively. The notation $\boldsymbol{x} \sim p(\cdot)$ means $\boldsymbol{x}$ sampled from $p(\cdot)$ and $\propto$ reads proportional to.

II. MODELING

We refer to the automated vehicle as the standard 1 trailer vehicle (S1T), because generally, there can be multiple trailers attached to the tractor. Other vehicles in the region of interest (ROI) of the S1T are designated as other vehicles (OV). Note that the OVs can be either autonomous or manual vehicles, and either moving or at standstill. Our method considers general discrete-time nonlinear vehicle models for describing the time evolution of the S1T,

$$\boldsymbol{x}_{k+1} = \bar{\boldsymbol{f}}(\boldsymbol{x}_k) + \bar{\boldsymbol{g}}(\boldsymbol{x}_k)\boldsymbol{u}_k, \tag{1}$$

with the state $\boldsymbol{x}_k \in \mathbb{R}^{n_x}$, input $\boldsymbol{u}_k \in \mathbb{R}^{n_u}$, and k is the time index corresponding to time t_k.

We introduce the following assumptions.

Assumption 1: Positions and velocities of the OVs relative to the EV at the current time are known.

The quantities involved in Assumption 1 can be measured and estimated by onboard sensors such as cameras, Lidars, radars, and/or ultrasound sensors attached to the EV. The future states of the OVs over the planning horizon are not assumed to be known a priori, but the prediction of the future state of OVs is incorporated into the planning method.

Assumption 2: The road geometry, number of lanes, and the direction of travel in each lane is known.

The quantities involved in Assumption 2 are usually known over the region of interest (ROI) from maps and onboard cameras. The relevant road information over the ROI is collected in the road state $\boldsymbol{x}^{\mathrm{RD}}$.

A. Vehicle Model for Motion Planning

A model based on force-mass balances is generally more accurate than a kinematic model, but for regular driving the differences are small. In this paper we use the discretized version of the kinematic S1T (Fig. 1) from [5],[1]

[1]Note that due to the different definition of the trailer angle θ, the equations of motion differ from [5].

$$\dot{\boldsymbol{x}} = \begin{bmatrix} \dot{p}_X \\ \dot{p}_Y \\ \dot{\delta}_s \\ \dot{\psi} \\ \dot{\theta} \\ \dot{v}_X \\ \dot{\phi}_s \end{bmatrix} = \begin{bmatrix} v_X \cos\psi \\ v_X \sin\psi \\ u_2 \\ \frac{1}{l} v_X \tan\delta_s \\ \Big[\frac{1}{b}\big(\frac{a}{l}\tan\delta_s\Big(\cos(\alpha) + \sin(\alpha)\tan(\phi_s)\Big) \\ -\Big(\sin(\alpha) - \cos(\alpha)\tan(\phi_s)\Big)\big)v_X\Big] \\ u_1 \\ u_3 \end{bmatrix} \tag{2}$$

where p_X, p_Y are the longitudinal and lateral position of the tractor rear wheel axle in the world frame, respectively, ψ is the heading (yaw) angle of the tractor, $\dot{\psi}$ is the yaw rate, θ is the heading (yaw) angle of the trailer, α is relative heading angle of the trailer given by $\alpha = \theta - \psi$, v_X is the longitudinal velocity of the tractor in the vehicle frame, δ_s is the steering angle of the front wheels of the tractor, ϕ_s is the steering angle of the trailer wheels, l is the wheel base, a is the distance from the rear tractor axle to the hitching point, and b is the distance from the trailer axle to the hitching point. The input u_1 is the tractor acceleration, u_2 is the front steering rate of the tractor at the road, and u_3 is the rear steering rate of the trailer at the road. Using the rates as inputs instead of the angles allows smooth steering and to constrain the rate of changes of the respective steering angle.

We impose various state and input constraints on the vehicle. The steering angles δ_s, ϕ_s, the steering rates $\dot{\delta}_s$, $\dot{\phi}_s$, and the acceleration $\dot{v}_X$ are subject to linear constraints, which can be compactly written as

$$\mathcal{U} = \{\boldsymbol{u}_k : \boldsymbol{u}_{\min} \leq \boldsymbol{u}_k \leq \boldsymbol{u}_{\max}\}. \tag{3}$$

The road-boundary constraint can be written as

$$\Gamma(p_X, p_Y) \leq 0, \tag{4}$$

where Γ is constructed from point-wise road data.

The constraints due to the OVs can take any shape. For instance, if the motion of the OVs is estimated by means of Kalman filters, a natural choice is to model the OVs as (conservative) ellipsoids. The spatial extent of the collision area of the S1T around the o-th OV is denoted with $\mathcal{B}_o$, and the corresponding OV state is $\boldsymbol{x}_o^{\mathrm{OV}} = [p_{X,o}^{\mathrm{OV}} \; p_{Y,o}^{\mathrm{OV}} \; \psi_o^{\mathrm{OV}} \; v_{x,o}^{\mathrm{OV}}]^{\mathrm{T}}$. We define the (deterministic or probabilistic) collision area at time step k as $\mathcal{O}_k(\boldsymbol{x}_{o,0}^{\mathrm{OV}}, \mathcal{B}_o)$, which depends on the measured/estimated OV state $\boldsymbol{x}_{o,0}^{\mathrm{OV}}$ at $k = 0$. Denote the planning horizon with T_f, the predicted collision area of the o-th OV for $k \in [0, T_f]$ is

$$\mathcal{S}_{k,o} = \mathcal{O}_{0:k}(\boldsymbol{x}_{o,0}^{\mathrm{OV}}, \mathcal{B}_o). \tag{5}$$

The area the motion planner should avoid up until time index k is computed as the union over all OV trajectory sets (5),

$$\mathcal{S}_k = \bigcup_{o=1}^{M} \mathcal{S}_{k,o}. \tag{6}$$

B. Driving Requirements

The proposed method is based on that nominal driving requirements can be determined a priori. These requirements can be summarized in the vector $\boldsymbol{y}_k \in \mathbb{R}^{n_y}$ for each time step k. We model the driving requirements to maintain a (possibly time varying) nominal velocity v_{nom}, be positioned in the middle of the lane corresponding to the driving mode, that is, to have zero deviation from the middle of the lane of both the tractor and the trailer, and ideally keep the distance larger than $d_{\min}$ from the surrounding vehicles.

The resulting trajectory from the motion planner will not exactly track $\boldsymbol{y}_k$, due to, e.g., conflicting requirements, input constraints, the vehicle kinematics limiting the drivable space, or sensing and modeling errors. The driving requirements are modeled as output equations on the vehicle states,

$$\hat{\boldsymbol{y}}_k = \boldsymbol{h}(\boldsymbol{x}_k, \mathcal{S}_k, \boldsymbol{x}^{\text{RD}}) + \boldsymbol{e}_k, \tag{7}$$

where $\boldsymbol{h}$ is a nonlinear function relating the S1T state $\boldsymbol{x}_k$, OV obstacle set $\mathcal{S}_k$ (hence also $\{\boldsymbol{x}^{\text{OV}}\}_{o=1}^{M}$), and road information $\boldsymbol{x}^{\text{RD}}$, to the driving requirements. Furthermore, $\boldsymbol{e}_k \in \mathbb{R}^{n_e}$ is the slack, which results in a probabilistic cost on the driving requirements. We model $\boldsymbol{e}_k$ as a stochastic Gaussian disturbance with covariance $\boldsymbol{R}_k$ according to $\boldsymbol{e}_k \sim (\boldsymbol{0}, \boldsymbol{R}_k)$, which may depend on the vehicle and driving mode. In this paper, we use the driving requirement function

$$\boldsymbol{h}(\boldsymbol{x}_k, \mathcal{S}_k, \boldsymbol{x}^{\text{RD}}) = \begin{bmatrix} v_{x,k} & p_{e,k} & q_{e,k} & d_{1,k} & \cdots & d_{M,k} \end{bmatrix}, \tag{8}$$

where $p_{e,k}$ and $q_{e,k}$ are the lateral deviations of the tractor and the trailer from the middle of the lane in the road-aligned frame, and $d_{j,k}$ is the distance to the jth obstacle.

We make the following assumption to incorporate the trailer constraint on $q_{e,k}$ into the driving requirements.

Assumption 3: The trailer heading angle θ or the relative angle of the trailer to the tractor $\alpha = \theta - \psi$, is known.

In practice, Assumption 3 does not exactly hold as θ or α are estimated online with some finite precision. However, we account for estimation errors by including uncertainty in the vehicle model and requirement function. From α and the dimensions of the S1T, we can determine the coordinates of any point on the trailer. In this paper, we determine the closest reference point from the middle of the lane to compute the lateral deviation of the trailer rear-axle point in the trailer's (local) frame of reference. The motion planner repeats this process at every time step in the planning and computes inputs that minimize this deviation while also trading-off with the other objectives.

III. Motion Planning Using Particle Filtering

The objective of our previously developed PF-based motion planner [19] is to determine an input trajectory and corresponding motion plan over the planning horizon T_f that navigates the road safely while satisfying input constraints (3), road constraints (4), and obstacle constraints (6). In addition, we want to minimize deviations from the predefined driving requirements (7).

In a Bayesian framework, by adding process noise $\boldsymbol{w}_k$ to the vehicle model (1), (1) and (7) can be formulated as

$$\boldsymbol{x}_{k+1} \sim p(\boldsymbol{x}_{k+1} | \boldsymbol{x}_k), \tag{9a}$$

$$\boldsymbol{y}_k \sim p(\boldsymbol{y}_k | \boldsymbol{x}_k, \boldsymbol{x}^{\text{RD}}, \mathcal{S}_k), \tag{9b}$$

where $\boldsymbol{x}_{k+1}$ and $\boldsymbol{y}_k$ are regarded as samples.

Given the vehicle dynamics (1), the goal of the motion-planning method is to generate an input trajectory $\boldsymbol{u}_k$, $k \in [0, T_f]$ over the planning horizon T_f satisfying the input constraints (3) such that the resulting trajectory obtained from (1) obeys (4), avoids the obstacle set (6), and reaches the goal region $\mathcal{X}_{\text{goal}}$, i.e., $\boldsymbol{x}_{T_f} \in \mathcal{X}_{\text{goal}}$, which is assumed to be given by a higher-level route planner.

The main idea in the approach is to determine the state trajectory PDF $p(\boldsymbol{x}_{0:T} | \boldsymbol{y}_{0:T}, \boldsymbol{x}^{\text{RD}}, \mathcal{S}_T)$, conditioned on the driving requirements $\boldsymbol{y}_{0:T}$ and the global information as a finite weighted sum over the planning horizon, and then to extract the trajectory from the PDF. By doing this iteratively, we construct a trajectory $\boldsymbol{x}_{0:T_f}$ based on the driving requirements. The driving requirements are the equivalent of sensor measurements in a traditional estimation problem.

We implement the motion planner in a receding horizon. The trajectory is computed for a time interval T_f but is only applied for $\Delta t \leq T_f$, and the maximum allowed (allocated) computation time for finding the motion plan is δt. We keep a committed tree, which is the part of the tree that will be executed. In the beginning of a planning phase, the measured S1T position is obtained, and the N1TT position over the allocated computation time δt is predicted, compared, and matched with a node being the closest node in the tree. Such node becomes the root node of the planning phase. The part of the tree that is not a descendant of the end node is deleted.

Algorithm 1 Proposed Planning Method

1: **Input:** State estimate $\hat{\boldsymbol{x}}$, goal region $\mathcal{X}_{\text{goal}}$, tree $\mathcal{T}$.
2: Propagate $\hat{\boldsymbol{x}}$ with the allocated time slot δt.
3: Set root node of $\mathcal{T}$ corresponding to $\hat{\boldsymbol{x}}$.
4: Delete part of $\mathcal{T}$ that is not a descendant of the root node.
5: Update obstacle set (6) and road constraint (4) to compute allowed region $\mathcal{X}_{\text{free}}$.
6: Set $t_{\text{CPU}} \leftarrow 0$
7: **while** $t_{\text{CPU}} \leq \delta t$ **do**
8:     Determine $\{\boldsymbol{x}_{0:T}, \boldsymbol{u}_{0:T-1}\}$ using a PF.
9:     **if** $\boldsymbol{x}_{0:T}$ is obstacle free **then**
10:         Add $\boldsymbol{x}_{0:T}$ as vertices $\mathcal{V}_{\text{new}}$ to $\mathcal{T}$.
11:         Add $\boldsymbol{u}_{0:T-1}$ as edges $\mathcal{E}_{\text{new}}$ to $\mathcal{T}$.
12:     **end if**
13: **end while**
14: Determine lowest-cost safe state trajectory $\boldsymbol{x}_{\text{best}}$ and corresponding controls $\boldsymbol{u}_{\text{best}}$.
15: Apply $\{\boldsymbol{x}_{\text{best}}, \boldsymbol{u}_{\text{best}}\}$ for time Δt, repeat from Line 1.

Algorithm 1 describes the planner. When the computation time exceeds δt, the safe trajectory with lowest accumulated cost C is chosen for execution (Line 15, Algorithm 1).

TABLE I

THE PARAMETER CHOICES FOR THE SIMULATION STUDY.

Parameter	Unit	Value	Meaning
N	-	100	# particles
Δt	s	0.5	Execution time
δt	s	0.1	Allocated computation time
T_s	s	0.1	Sampling period motion planner
T_f	s	10	Planning horizon
h	ms	25	Controller sampling period
T	-	T_f/T_s	Prediction time
d_{min}	m	4	Safety distance
$\delta_{\max}$ ($\phi_{\max}$)	deg	15	Maximum steering angle
$\dot{\delta}_{\max}$ ($\dot{\phi}_{\max}$)	deg/s	10.5	Maximum steering rate
$\dot{v}_{X,\max}$	m/s^2	0.5	Maximum acceleration

IV. RESULTS

This section presents and analyzes results from simulations in scenarios of a tractor-trailer combination traveling in obstacle-free environments, when confronted with OVs in the same lane, and during tight turning.

A. Parameters

Table I shows the different parameters in the planner, symmetric input constraints, and symmetric state constraints. The planner replans a $T_f = 10$s trajectory every $= 0.5$s, with an alloted computation time $\delta t = 0.1$s. In this way, we account that while the sensors can detect long-range obstacles over the planning horizon T_f, they are more reliable for shorter distances (corresponding to Δt). The discretization period of the dynamics is $T_s = 0.1$s.

The cost for each node in the tree $\mathcal{T}$ can be chosen differently, e.g., as a distance from the goal, the offset from a nominal path, the offset from a nominal velocity, the distance to OVs, or a combination thereof. In the current implementation we penalize the offset from the nominal velocity, the tractor's and the trailer's deviation from the lane center, and the distance to OVs located less than a safety distance d_{min} from the ego vehicle. The $\boldsymbol{Q}$ and $\boldsymbol{R}$ used are

$$\begin{aligned}\boldsymbol{Q} &= \operatorname{diag}(1^2, (\frac{100\pi}{180})^2, (\frac{100\pi}{180})^2),\\ \boldsymbol{R} &= \operatorname{diag}(2^2, 1^2, 1^2, 0.2^2)\end{aligned} \tag{10}$$

where $\operatorname{diag}(.)$ denotes a diagonal matrix.

B. Results in Highway Driving Scenario

Fig. 2 displays four snapshots of an excerpt of a situation where a vehicle is located in front of the EV, in the same lane, which necessitates a lane change. Subsequently, the proposed method successfully plans a new trajectory for the EV to change lane. In particular, at ($t = 21$s), the planner observes the obstacle and computes a smooth path to change lane. At all times, the planner is trading off between minimizing deviation of the tractor and trailer rear-axle midpoint from the centerline of the road segment, and tracking the reference velocity as close as possible. From ($t = 23$s) to ($t = 27$s), the vehicle successfully overtakes the OV.

Figs. 3 and 4 display results when the motion planner is executing in closed loop with a high-level decision maker and a low-level tracking controller, similar to [20]. Fig. 3 shows a comparison of the planned and attained velocities, as well as the trajectories when the articulated vehicle comes to a stop from a certain initial nominal velocity, and Fig. 4 displays a comparison of the planned and attained velocities, as well as the trajectories when the articulated vehicle takes a sharp turn. In both cases, the controller successfully tracks the velocity references determined by the motion planner. Secondly, Figs. 3 and 4 also present the corresponding tracking error between the reference path computed by Algorithm 1 and the actual trajectory driven by the vehicle. The tracking error remains smaller than 10cm in all of the above scenarios, indicating that the motion planner determines realistic trajectories, even in sharp turns, which can be closely followed by a low-level controller.

C. Impacts of Active Trailer Steering in Cornering

To validate impact of the active trailer steering in the motion planning, we evaluate the swept path with and without trailer steering for a turning maneuver consisting of; (i) driving a straight-line section; (ii) performing a 270 deg turn to the right; and (iii) driving straight again. The swept path is defined by the outer path of the tractor front wheel axle and the path of the center of the trailer wheel axle.

Fig. 5 shows the resulting swept paths with and without trailer steering. Irrespective of using active or passive trailer, both configurations manage to plan a path closely following the middle of the lane (indicated in dashed). However, for the passive trailer configuration, the trailer due to lack of controllability will follow the planning enforced for the tractor. For the case of active trailer, however, the planner manages to decrease the deviations from the middle of the lane, although to exactly plan a path for both the tractor and trailer is not feasible due to input constraints and the dimensions of the trailer. Here, note that it is possible to trade off deviations of the tractor to deviations of the trailer, but in this particular simulation the cost function was chosen to prioritize the tractor mid-lane deviations.

Fig. 6 displays the deviation of the trailer to the middle of the lane, corresponding to the planned trajectories in Fig. 5. Overall, the active trailer reduces the mid-lane deviations in the planning from about 5m to 1.5m.

V. CONCLUSION

We extended our previously proposed PF-based motion planner [19] from passenger vehicles to a tractor-trailer combination with active trailer steering. The method formulates the motion-planning problem as a nonlinear stochastic estimation problem and therefore by construction accounts for environmental and modeling uncertainties. We showed that the method is suitable for online motion planning of articulated vehicles and that the generated trajectories are dynamically feasible and can be closely tracked by a subsequent low-level controller. Our results indicate that the planner provides drivable trajectories for a number of different scenarios, such as lane following, lane change and obstacle avoidance. In addition, by having active trailer steering, the

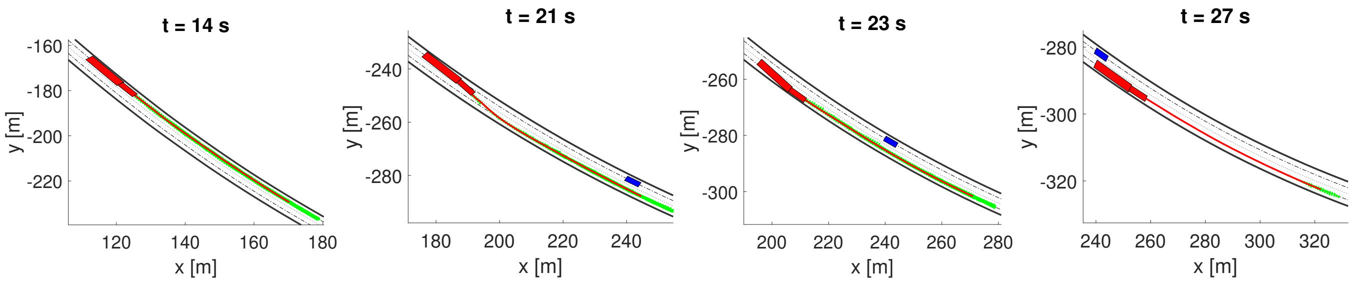

Fig. 2. Four snapshots from a simulation of a tractor-trailer combination overtaking a stand-still OV.

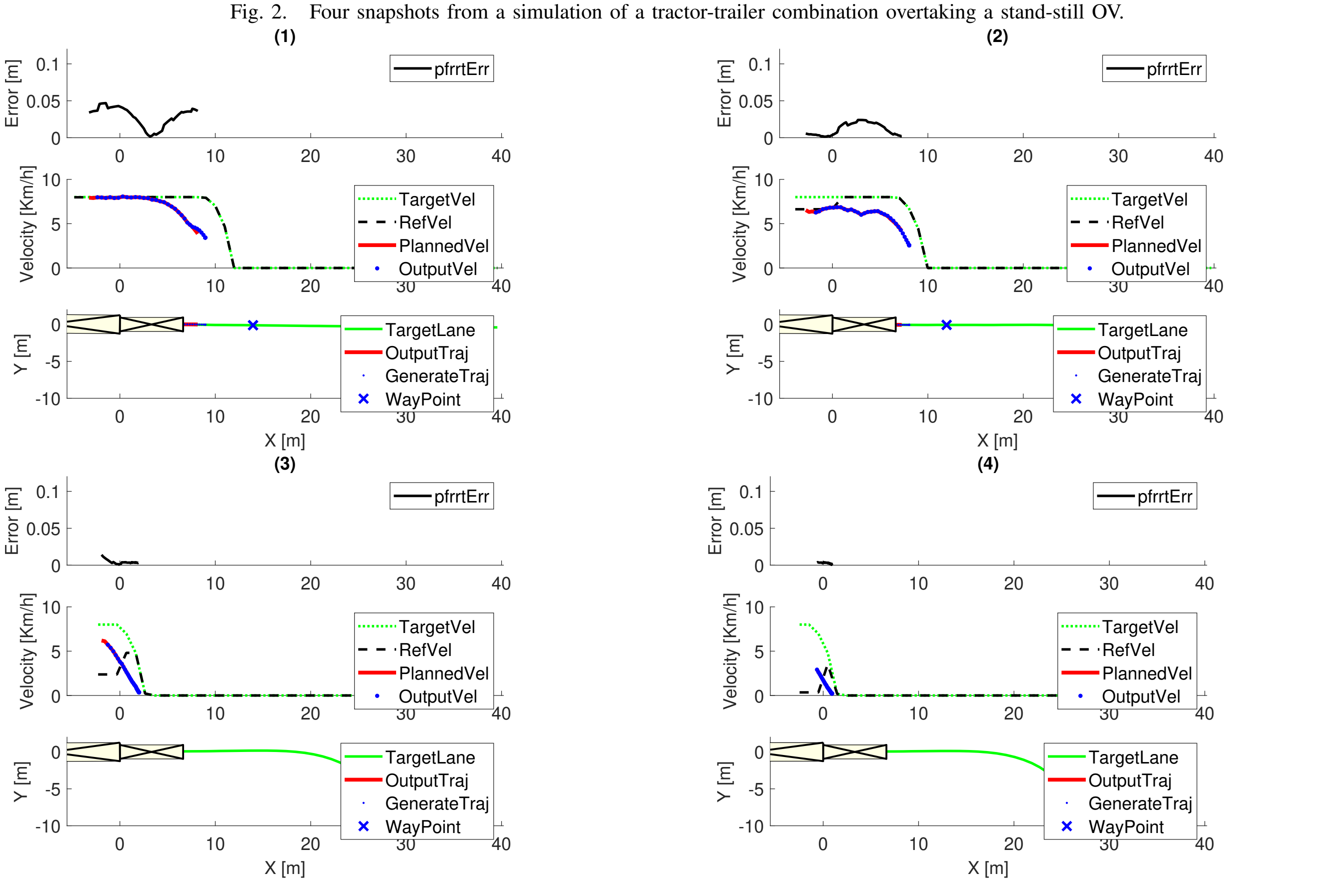

Fig. 3. Results when Algorithm 1 runs in closed-loop with a high-level decision maker and low-level tracking controller. The plots show the tracking error, reference, planned and actual velocities, and trajectories when the vehicle is coming to a stop.

motion plans determined by our planner substantially reduce the swept path compared to passive trailer steering.

References

[1] S. M. Broek, E. van Nunen, and H. Zwijnenberg, "Definition of necessary vehicle and infrastructure systems for automated driving," Eur. Commission, Tech. Rep. 2010/0064, Jun. 2011.

[2] P. Fancher and C. Winkler, "Directional performance issues in evaluation and design of articulated heavy vehicles," *Vehicle System Dynamics*, vol. 45, no. 7-8, pp. 607–647, 2007.

[3] O. Ljungqvist, "Motion planning and feedback control techniques with applications to long tractor-trailer vehicles," Ph.D. dissertation, Linköping University, 2020.

[4] K. Berntorp, "ESP for suppression of jackknifing in an articulated bus," Department of Automatic Control, Lund University, Sweden, Master's Thesis ISRN LUTFD2/TFRT--5831--SE, Dec. 2008.

[5] P. Ritzen, E. Roebroek, N. van de Wouw, Z.-P. Jiang, and H. Nijmeijer, "Trailer steering control of a tractor–trailer robot," *IEEE Transactions on Control Systems Technology*, vol. 24, no. 4, pp. 1240–1252, 2016.

[6] N. Murgovski and J. Sjöberg, "Predictive cruise control with autonomous overtaking," in *Conf. Decision and Control*, 2015, pp. 644–649.

[7] V. Turri, A. Carvalho, H. E. Tseng, K. H. Johansson, and F. Borrelli, "Linear model predictive control for lane keeping and obstacle avoidance on low curvature roads," in *Int. Conf. Intell. Transporations Systems*, 2013, pp. 378–383.

[8] S. M. LaValle, *Planning algorithms*. Cambridge university press, 2006.

[9] Y. Kuwata, J. Teo, G. Fiore, S. Karaman, E. Frazzoli, and J. P. How, "Real-time motion planning with applications to autonomous urban driving," *IEEE Trans. Control syst. Technol.*, vol. 17, no. 5, pp. 1105–1118, 2009.

[10] C. Urmson, J. Anhalt, D. Bagnell, C. Baker, R. Bittner, M. Clark, J. Dolan, D. Duggins, T. Galatali, C. Geyer *et al.*, "Autonomous driving in urban environments: Boss and the urban challenge," *J. field Robot.*, vol. 25, no. 8, pp. 425–466, 2008.

[11] M. Montemerlo, J. Becker, S. Bhat, H. Dahlkamp, D. Dolgov, S. Ettinger, D. Haehnel, T. Hilden, G. Hoffmann, B. Huhnke *et al.*, "Junior: The stanford entry in the urban challenge," *Journal of field Robotics*, vol. 25, no. 9, pp. 569–597, 2008.

[12] A. Stentz *et al.*, "The focussed d^* algorithm for real-time replanning," in *IJCAI*, vol. 95, 1995, pp. 1652–1659.

[13] S. Koenig and M. Likhachev, "Fast replanning for navigation in unknown terrain," *IEEE Trans. Robot.*, vol. 21, no. 3, pp. 354–363, 2005.

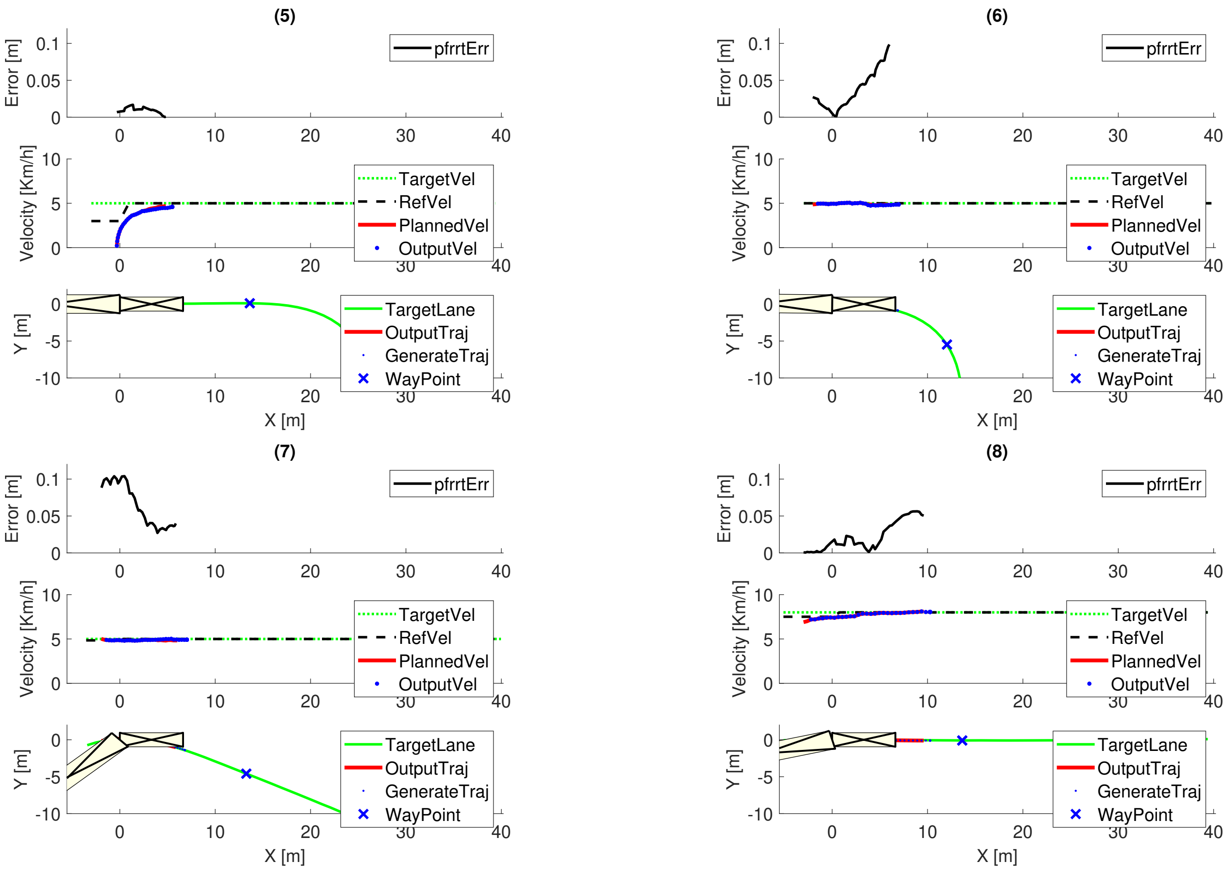

Fig. 4. Results when Algorithm 1 runs in closed-loop with a high-level decision maker and low-level tracking controller. The plots display the tracking error, reference, planned and actual velocities, and trajectories when vehicle is taking a sharp turn.

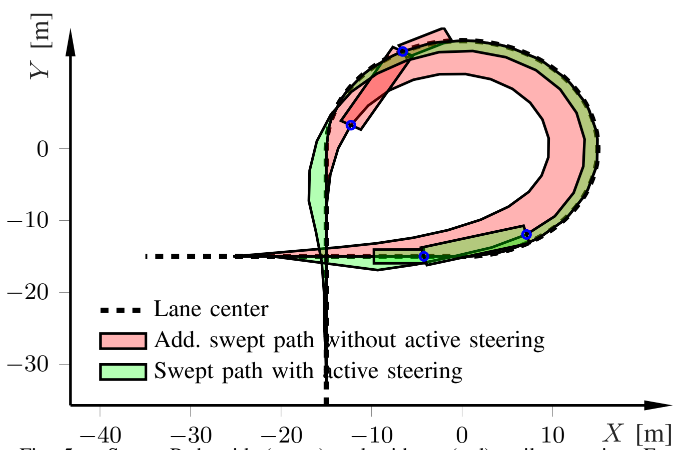

Fig. 5. Swept Path with (green) and without (red) trailer steering. For illustration purposes, we display a snapshot of the tractor-trailer configuration for both cases.

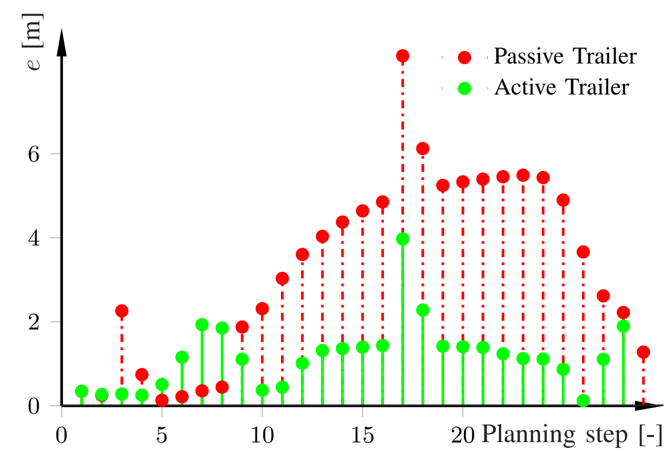

Fig. 6. Lateral deviation of the planned trailer trajectory with (green) and without (red) trailer steering throughout the maneuver in Fig. 5. The lateral deviation is determined from the center of the trailer wheel axle.

[14] S. J. Anderson, S. C. Peters, T. E. Pilutti, and K. Iagnemma, "An optimal-control-based framework for trajectory planning, threat assessment, and semi-autonomous control of passenger vehicles in hazard avoidance scenarios," *Int. J. Veh. Auton. Syst.*, vol. 8, no. 2-4, pp. 190–216, 2010.

[15] K. Berntorp, "Path planning and integrated collision avoidance for autonomous vehicles," in *Amer. Control Conf.*, 2017, pp. 4023–4028.

[16] R. Oliveira, O. Ljungqvist, P. F. Lima, and B. Wahlberg, "Optimization-based on-road path planning for articulated vehicles," vol. 53, no. 2, pp. 15 572–15 579, 2020, 21st IFAC World Congress.

[17] N. Evestedt, O. Ljungqvist, and D. Axehill, "Motion planning for a reversing general 2-trailer configuration using closed-loop rrt," in *Int. Conf. Intell. Robots and Systems*, 2016, pp. 3690–3697.

[18] S. Beyersdorfer and S. Wagner, "Novel model based path planning for multi-axle steered heavy load vehicles," in *Int. Conf. Intell. Transp. Syst.*, 2013, pp. 424–429.

[19] K. Berntorp, T. Hoang, and S. Di Cairano, "Motion planning of autonomous road vehicles by particle filtering," *IEEE Trans. Intell. Veh.*, vol. 4, no. 2, pp. 197–210, 2019.

[20] K. Berntorp, T. Hoang, R. Quirynen, and S. Di Cairano, "Control architecture design of autonomous vehicles," in *Conf. Control Technol. and Applications*, Copenhagen, Denmark, Aug. 2018, invited paper.